INVESTIGATIONS AND COMPUTER SIMULATIONS OF THE INTERGRAIN DIFFUSION IN SUBMICRO- AND NANOCRYSTALLINE METALS

Yu. R. Kolobov[1], A. G. Lipnitskii[1], I. V. Nelasov[1], and G. P. Grabovetskaya[2]

Investigations of the features of the diffusion along grain boundaries and of the diffusion-controlled processes in submicroscopic and nanocrystalline materials produced by methods of intense plastic deformation are reviewed. To determine the parameters of the diffusion along grain boundaries and triple junctions in metals, which are independent of the results of processing of diffusion experiments based on diffusion models, results of a molecular dynamic investigation of the diffusion in nanocrystalline copper considered as an example are presented. Comparison of the features of grain boundary diffusion in submicroscopic and nanocrystalline materials produced by various methods is performed.

INTRODUCTION

Submicrocrystalline (SMC) (grain size 100 nm < d < 1 μm) and nanocrystalline (NC) (d << 100 nm) metals and alloys are promising structural and functional materials in modern engineering [1, 2]. The small grain size and, hence, extended internal interfaces (boundaries of grains, subgrains, and second phases) dictate the necessity of studying the mechanism of grain boundary diffusion in these materials. This is related to that the diffusion-controlled grain boundary processes play an important, sometimes dominant part in the development of plastic deformation, structural degradation, and destruction of metal polycrystals [3]. A rather great body of theoretical and experimental data on the diffusion properties of submicrocrystalline and nanocrystalline materials has been gained in the literature [4–12] to date. Specialized phenomenological models of the grain boundary diffusion in these materials have been developed [13–16]. Classification of modes of grain boundary diffusion has been made [14]. Unfortunately, only few reviews are available in the scientific literature that are devoted to the mechanisms of diffusion and diffusion-controlled processes in submicrocrystalline and nanocrystalline materials in comparison to the corresponding features of these processes developing in conventional polycrystals. Reviews of the computer simulations of the processes under consideration occurring in submicrocrystalline and nanocrystalline materials are not available. In this connection, the present review considers the above problems based on the authors' original results and on the data available in the literature.

RESULTS OF DIRECT EXPERIMENTAL AND THEORETICAL STUDIES OF GRAIN BOUNDARY DIFFUSION IN SMC AND NC METALS

Experimental studies of grain boundary diffusion in SMC materials were carried out in the main with SMC metals produced by intense plastic deformation [8–12, 17–19]. The parameters of grain boundary diffusion (diffusion coefficients and activation energies) were obtained, as a rule, from the experimental depth distribution profiles of the layer concentration or concentration in a grain boundary (GB) of the diffusant (an impurity or an isotope) after diffusion

TABLE 1. Coefficients of Grain Boundary and Bulk Diffusion in SMC and NC Metals Treated by Intense Plastic Deformation

Material	d, nm	Diffusant	T, K	D, m^2/s			Reference
				D_n	D_b	D_v	
Ni	270	Cu	398	$5.06\cdot10^{-15}$	$4.64\cdot10^{-20}$	$1.4\cdot10^{-34}$	[10]
	270	Cu	423	$9.6\cdot10^{-15}$	$4.31\cdot10^{-19}$	$1.4\cdot10^{-32}$	
	270	Cu	443	$2.2\cdot10^{-14}$	$2.14\cdot10^{-18}$	$3.7\cdot10^{-31}$	
Ti	320	Co	423	$8.4\cdot10^{-15}$	$9.0\cdot10^{-17}$	$1.56\cdot10^{-20}$	[18]
	320	Co	448	$1.7\cdot10^{-14}$	$3.6\cdot10^{-16}$	–	
	320	Co	473	$4.1\cdot10^{-14}$	$2.0\cdot10^{-15}$	$4.8\cdot10^{-19}$	
Pd	80–150	^{59}Fe	371	$1.0\cdot10^{-21}$	$8.0\cdot10^{-25}$	–	[9]
	80–150	^{59}Fe	401	$3.0\cdot10^{-20}$	$1.2\cdot10^{-23}$	–	
	80–150	^{59}Fe	473	$5.0\cdot10^{-20}$	$6.0\cdot10^{-21}$	–	
	80–150	^{59}Fe	577	$9.0\cdot10^{-20}$	$3.0\cdot10^{-18}$	–	
Fe	150	^{59}Fe	528	$4.0\cdot10^{-19}$	$1.0\cdot10^{-19}$	–	[11]
Mo	450	Ni	973	$1.0\cdot10^{-13}$	$1.5\cdot10^{-16}$		[19]
	450	Ni	1073	$4.4\cdot10^{-13}$	$2.6\cdot10^{-15}$		
	450	Ni	1123	$7.8\cdot10^{-13}$	$8.7\cdot10^{-15}$		

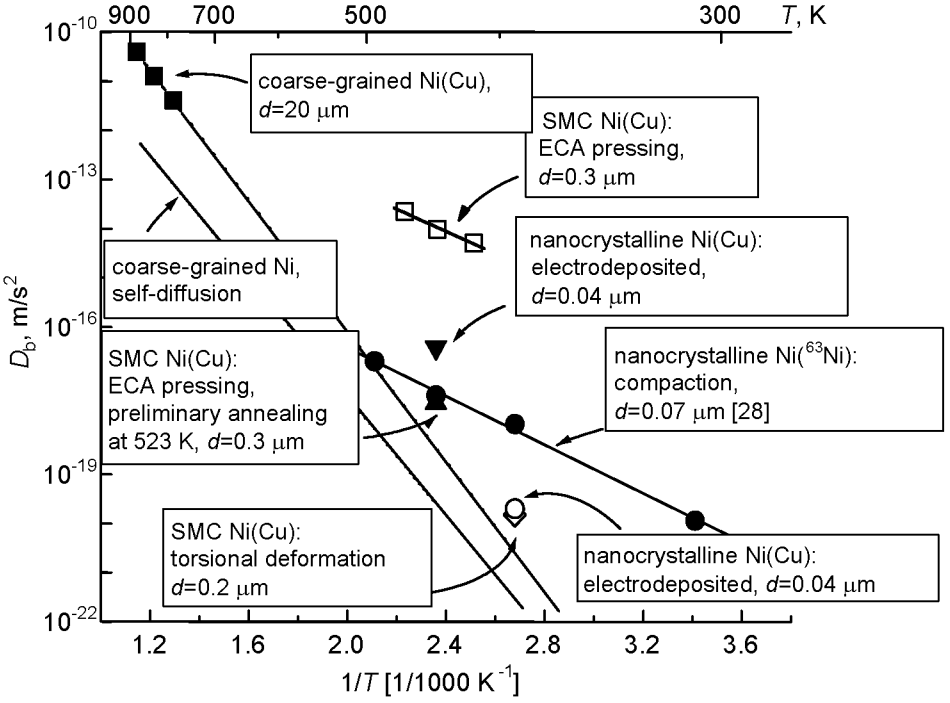

Fig. 1. Arrhenius temperature dependence of the coefficients of grain boundary diffusion of copper in nickel of varied structure [17].

annealing under the conditions in which bulk diffusion "is frozen" and there is no outflow of the diffusant from the grain boundary to its bulk. The principal results of these investigations are presented in Fig. 1 and in Table 1. Herein, for comparison, the corresponding values of grain boundary diffusion coefficients D_b and their temperature dependence for coarse-grained polycrystals are given.

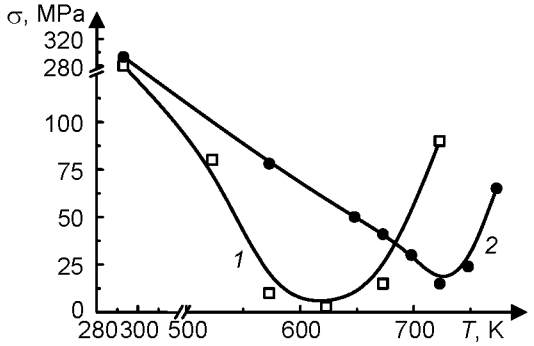

Fig. 2. Temperature dependence of the flow stress for an UFG (curve *1*) and for a fine-grained Al–Mg–Li–Zr alloy (curve *2*) under optimum superplasticity conditions [20].

From Fig. 1 and Table 1 it can be seen that the D_b values for polycrystals in coarse-grained and SMC states can coincide or differ by 1–5 orders of magnitude, and the D_b values obtained at the same temperature in different experiments vary within 2–3 orders of magnitude. The values of the activation energy for grain boundary diffusion, Q_b, in the SMC metals, determined from the temperature dependence of D_b [10, 17–19], turned out to be lower by a factor of 1.5–2 than the corresponding values for the coarse-grained state and close to the values of the activation energy for free surface diffusion.

Since there was a significant spread in experimental values of D_b for SMC metals, it was of interest to obtain indirect estimates of this quantity from the data of studies of diffusion-controlled processes in SMC, ultrafine-grained (UFG), fine-grained and coarse-grained polycrystals.

It is well known that the basic deformation mechanism in superplastic flow is grain boundary sliding controlled by GB diffusion. Using experimental data on the temperature dependence of the flow stress obtained for UFG and fine-grained superplastic alloys, one can estimate the difference in diffusion parameters of an alloy in the mentioned states. Figure 2 presents the temperature dependence of the flow stress for a superplastic alloy of the Al–Mg–Li–Zr system in an UFG state, obtained by the method of equal-channel angle pressing, and in a fine-grained state [20]. These curves show a minimum corresponding to the optimum conditions for superplasticity and to the maximum elongation before rupture. It can be seen that for the UFG state of the alloy the optimum temperature at which superplasticity shows up shifts to the lower temperatures by ~100 K. The superplastic flow of the alloy is described rather well by the expression [21]

$$\dot{\varepsilon} = A\frac{D^{\text{eff}}}{kT}\sigma^2\frac{1}{d^2}, \tag{1}$$

where A is a constant, D^{eff} is the effective diffusion coefficient, σ is the applied stress, and d is the grain size.

Substituting the grain size (10 and 1 μm for the fine-grained and the UFG state, respectively), the stresses (the values corresponding to the minimum in Fig. 2), and the velocity of superplastic flow ($5\cdot10^{-4}$ and 10^{-2} s^{-1} for the fine-grained and the UFG state, respectively [20]) and assuming that the coefficient A depends on structure, we can estimate the ratio of the effective diffusion coefficients:

$$\frac{D^{\text{eff}}_{\text{FG}}\,(T = 723\text{ K})}{D^{\text{eff}}_{\text{UFG}}\,(T = 623\text{ K})} \sim 1.$$

Thus, the effective diffusion coefficients are approximately equal for the mentioned states, despite the 100-K difference in temperatures. Supposing that the activation energy in the Arrhenius law by which the diffusion coefficient varies corresponds to the superplastic flow activation energy for the Al–Mg–Li–Zr alloy (Q = 145 kJ/mol), we obtain

$$D_{\mathrm{FG}}^{\mathrm{eff}}(623\ \mathrm{K}) = 2\cdot 10^{-2} D_{\mathrm{UFG}}^{\mathrm{eff}}(723\ \mathrm{K}) .$$

From the expressions above it follows that the effective diffusion coefficient for the UFG state is greater than that for the fine-grained state by approximately two orders of magnitude.

The authors of Ref. 22 have estimated the coefficients D_{b} for diffusion of nickel in SMC molybdenum by the results of an investigation of the kinetics of activated recrystallization (AR) in molybdenum. Activated recrystallization takes place at a lower metal temperature under the conditions of diffusion of substitutional impurity atoms from the environment (coating) [23]. The reason for the activated recrystallization of metals is the presence of uncompensated GB diffusion flows of impurity atoms which give rise to GB stresses and thus transfer the GB in a nonequilibrium high-energy state. A consequence of this is the enhanced mobility of the GB's [3]. The AR process is controlled by diffusion. The kinetics of the increase of the thickness h of the recrystallized layer, which is formed at the very beginning of the AR process in a thin near-surface layer at later stages and which can be observed not only in a scanning electron microscope, but also in an optical one, is described by the equation

$$h = At^{1/2}, \tag{2}$$

where t is time and A is a constant.

It has been shown [24] that AR occurs in GB's if a nonstationary diffusion mode of the **C**-type (following the classification given elsewhere [25]) or a $\mathbf{B}_1$-type mode (similar by conditions to a **C**-type one) is realized. The **C** mode corresponds to GB diffusion with no outflow of the impurity in the bulk of grains. In the $\mathbf{B}_1$ mode, outflow of the impurity in the grain bulk begins. The motion of the activated recrystallization front is controlled by grain boundary diffusion and depends on the depth of penetration of the diffusant in the metal.

According to the Fisher model, the impurity concentration $C(x, y, z)$ in a GB at a depth $\boldsymbol{x}$ can be determined by solving the equation [26]

$$\frac{\partial C_{\mathrm{b}}}{\partial t} = D_{\mathrm{b}}\frac{\partial^2 C_{\mathrm{b}}}{\partial y^2} + \frac{2D_V}{\delta}\frac{\partial C_V}{\partial x}, \tag{3}$$

where D_{b} is the grain boundary diffusion coefficient, δ is the width of the GB, D_V is the bulk diffusion coefficient, and t is time.

The second term in Eq. (3) describes the impurity outflow in the grain bulk, and it is absent for the **C** mode. For this case, the solution of Eq. (3) for the mean square displacement of atoms along the GB will be same as for bulk diffusion [25], and the depth of penetration of the impurity in the material bulk in the mode **C** will be described as a first approximation by the expression

$$x^2 = 2D_{\mathrm{b}}t . \tag{4}$$

Thus, investigating the AR kinetics, one can judge on the diffusion penetrability of the GB and make indirect estimates of the parameters of the grain boundary diffusion.

For ultrafine-grain metals and alloys, the classification of grain boundary diffusion modes has been refined [14]. It was proposed to term formally the **C**, $\mathbf{B}_1$, and $\mathbf{B}_2$ modes as **C**′, $\mathbf{B}_1$′, and $\mathbf{B}_2$′ modes, respectively, if the diffusant penetration depth is greater than the grain size (d). Thus the GB diffusion **C** mode is observed if $(D_V t)^{1/2} << s\delta/2 << d << (D_{\mathrm{b}}t)^{1/2}$. To a type-**B** mode there corresponds the condition $s\delta/2 << (D_V t)^{1/2} << d << (D_{\mathrm{b}}t)^{1/2}$. In view of the diffusant outflow from GB's perpendicular to the surface, expressions for the depth of penetration of the impurity along GB's have been found for inclined GB's for the **C** mode and for type-**B** modes, respectively [14]:

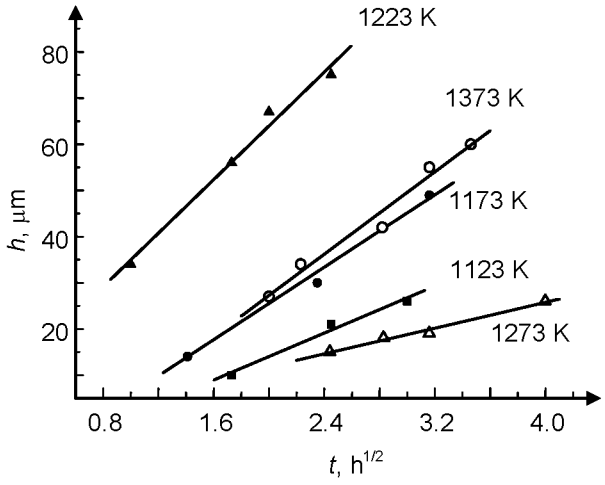

Fig. 3. The width of the recrystallized layer as a function of the time of diffusion annealing for a Mo(Ni) SMC system, solid symbols (*a*), and for a Mo (Ni) fine-grained system, open symbols (*b*).

$$x = (D_b t)^{1/2} \tag{5}$$

and

$$x = \frac{(s\delta D_b)^{1/2}}{(4D_V / t)^{1/4}}, \tag{6}$$

where s is the coefficient of segregation.

In the $\boldsymbol{B}_1$ mode the grain bulk diffusion will affect the depth of penetration of the impurity in the bulk of the specimen and, hence, the development of AR. At the same time, the effective diffusion coefficient in this case inappreciably differs from the grain boundary diffusion coefficient [14].

Figure 3 presents the kinetic curves showing the variation of the recrystallized layer width (h) for a Mo(Ni) system in the fine-grained state (grain size ~5 μm) and in the SMC state (size of the elements of the grain-subgrain mixture 0.2–0.5 μm) (hereinafter the diffusant impurity is specified in parentheses) at temperatures of 1273 and 1373 K for fine-grained molybdenum and 1123, 1173, and 1223 K for SMC molybdenum [22]. It can be seen that the relation $h(t)$ fits Eq. (2) for any temperature. Based on the data given in Fig. 3, the activation energy of the AR process (Q_{AR}) has been estimated (Table 1). The Q_{AP} value obtained (263 ± 20 kJ/mol) is close to the values of the activation energy of activated recrystallization for molybdenum-base alloys (Q_{AR} = 272 kJ/mol [27]) and it is somewhat greater than the activation energy of the grain boundary diffusion of nickel in molybdenum (Q_b = 210 kJ/mol [28]). The greater value of the activation energy of the AR process compared to Q_b seams to be related to that AR can include processes related to bulk diffusion, such as the formation and climb of lattice dislocations near migrating GB's [29].

Table 2 lists the values of D_b for SMC molybdenum at temperatures of 1223–1123 K calculated from the width of the AR front by Eqs. (5) and (6). The calculation of D_b with the use of Eq. (6) has been performed for δ = 10 nm [30] and s = 1. (It is well known [28] that when GB's migrate, the impurity which is present in the GB's remains in the grain bulk; therefore, the impurity concentration in the GB's and in the adjacent region is approximately the same, and, hence, $s \sim 1$.) From Table 2 it can be seen that at the temperatures at which the probability of the impurity outflow from GB's in the grain bulk is high (1223 and 1173 K), the values of D_b for SMC molybdenum calculated by Eqs. (5) and (6) vary within the error of measurement of the AR layer width. Comparison of the D_b values for fine-grained molybdenum and for SMC molybdenum calculated by the width of the AR layer shows that the D_b values for SMC molybdenum at

TABLE 2. Coefficients of Diffusion of Nickel in Molybdenum [22]

Temperature	Fine-grained Mo D_b, m^2/s	Coarse-grained Mo D_b, m^2/s [19]	SMC Mo D_b, m^2/s, Eq. (5)	SMC Mo D_b, m^2/s, Eq. (6)
1373	$3.1 \cdot 10^{-14}$ (exper.)	$1 \cdot 10^{-12}$		
1273	$5.6 \cdot 10^{-15}$ (exper.)	$1.9 \cdot 10^{-13}$		
1223	$2.2 \cdot 10^{-15}$ (calc.)		$2.6 \cdot 10^{-13}$	$1.2 \cdot 10^{-13}$
1173	$7.5 \cdot 10^{-16}$ (calc.)		$6.6 \cdot 10^{-14}$	$1.9 \cdot 10^{-14}$
1123	$2.3 \cdot 10^{-16}$ (calc.)		$2.0 \cdot 10^{-14}$	$2.1 \cdot 10^{-15}$

TABLE 3. Grain Boundary Diffusion Coefficients D_b for Coarse-Grained and SMC Titanium [18]

Temperature, K	Coarse-grained titanium	SMC titanium	SMC titanium + annealing (673 K, 1 h)
423	$9.1 \cdot 10^{-17}$	$8.4 \cdot 10^{-15}$	$6.4 \cdot 10^{-17}$
448	$3.6 \cdot 10^{-16}$	$1.7 \cdot 10^{-14}$	$3.2 \cdot 10^{-16}$
473	$2.0 \cdot 10^{-15}$	$4.2 \cdot 10^{-14}$	10^{-15}
523	$1.9 \cdot 10^{-14}$	$1.8 \cdot 10^{-13}$	$1.4 \cdot 10^{-14}$

temperatures of 1223–1123 K are two orders of magnitude greater than the corresponding D_b values for fine-grained molybdenum. (The D_b values for fine-grained molybdenum at 1223–1123 K have been calculated by the Arrhenius equation based on the AR data obtained at temperatures of 1373 and 1273 K.)

Comparison of the D_b values for nickel in SMC molybdenum determined directly from the depth of penetration of nickel along the GB's of molybdenum (Table 1) and by an indirect method from the width of the AR layer (Table 2) has shown that the D_b values determined by the indirect method for a temperature of 1123 K (Table 1) are two orders of magnitude lower than the corresponding D_b values determined from the Auger spectrometry data on the depth of penetration of nickel in molybdenum along immobile GB's [19]. At the same time, the difference in D_b values between SMC and coarse-grained molybdenum at the mentioned temperature is two orders of magnitude for both methods.

Numerous investigations show that the SMC structure of metallic materials produced by intense plastic deformation methods, features, besides a small grain size, an extremely nonequilibrium GB's. In this state, the grain boundaries have a high density of deformation-induced defects, possess an elevated energy and an excess volume compared to the minimum ones for given conditions, and produce long-range elastic stress fields and distortion of the crystal lattice in the near-boundary region [1, 30]. The degree of nonequilibrium of the GB's in a submicrocrystalline material is determined by the properties of the material and by the method and mode of its production. Therefore, the variations in D_b values obtained at the same temperature in different experiments can be related to the varied degree of nonequilibrium of the GB's in the metals under investigation.

The effect of the GB state on the diffusion properties of submicrocrystalline metals was investigated for SMC titanium and molybdenum [18, 19]. A well-controlled method for changing the state of the defect structure of GB's in SMC metals produced by intense plastic deformation (IPD) is to realize the processes of relaxation of elastic stresses and reduction of the defect density in GB's and near-boundary regions by preliminary annealing of the SMC metal at temperatures below its recrystallization temperature [1]. The state of GB's in SMC titanium was changed by pre-recrystallization annealing of the metal at 623 K for 1 h before the deposition of cobalt on its surface. This annealing, not changing the grain size, transfers the GB's in SMC titanium to the equilibrium state [18]. The values of D_b for cobalt in SMC titanium in the original state, after IPD, and after annealing in the mentioned mode are given in Table 3. It can be seen that preliminary annealing reduces D_b for cobalt in SMC titanium by 1–2 orders of magnitude, depending on the temperature of diffusion annealing.

The state of GB's in SMC molybdenum was changed by preliminary annealing of the metal at a temperature of 1023 K for 2 h before the deposition of nickel on its surface [19]. After this annealing, a decrease in dislocation density and the appearance of streaky contrast on the GB's, characteristic of equilibrium GB's, are observed in submicrocrystalline molybdenum with the mean size of grain-subgrain structure elements remaining unchanged.

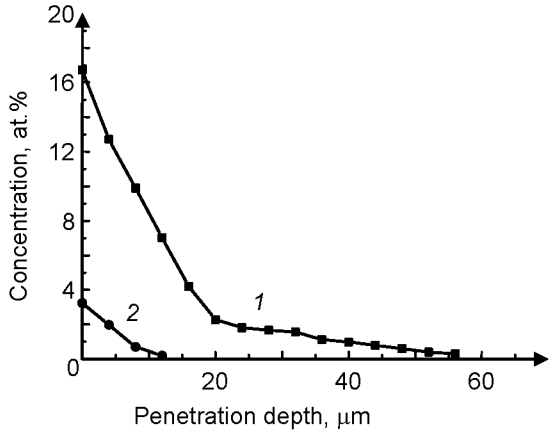

Fig. 4

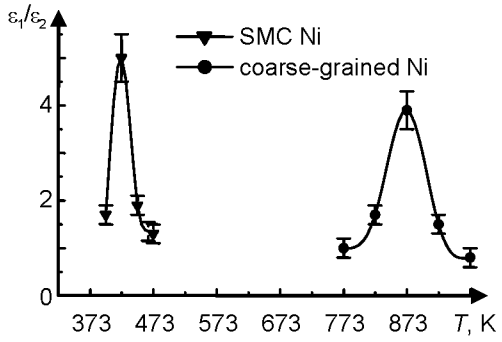

Fig. 5

Fig. 4. Concentration profiles of depth distribution of nickel in grain boundaries of submicrocrystalline molybdenum after diffusion annealing at 1073 K for 2 h: molybdenum in the state after IPD (curve *1*); molybdenum in the state after IPD + annealing at 1023 K for 2 h (curve *2*) [19].

Fig. 5. Creep speed-up effect in coarse-grained and submicrocrystalline nickel under the action of diffusion flows of copper atoms from the coating.

Figure 4 presents the concentration profiles of nickel distribution in GB's for original and pre-annealed submicrocrystalline molybdenum after diffusion annealing at 1073 K for 2 h. It can be seen that the depth of penetration of nickel along GB's in pre-annealed submicrocrystalline molybdenum decreased by a factor of ~4.5 compared to that in the original state, and D_b decreased to $6.8 \cdot 10^{-15}$ m^2/s, which is close to the value corresponding to the coarse-grained state ($3.3 \cdot 10^{-15}$ m^2/s).

The significant effect of the state of GB's on the parameters of grain boundary diffusion and on diffusion-controlled processes in SMC materials produced by IPD is demonstrated by the data [1, 31, 32] obtained in studies of the effect of diffusion flows of substitutional impurity atoms from the surface on the creep of SMC metals. It is well known [3, 33] that the action of grain boundary diffusion flows on GB's in polycrystals and in bicrystals gives rise to effects initiated by AR diffusion, to migration of grain boundaries, and to grain-boundary sliding. It has been shown [34] that under certain conditions the activation of grain-boundary sliding (GBS) by grain boundary diffusion flows of substitutional impurity atoms can significantly reduce the creep resistance.

Even first investigations [31] performed with SMC nickel produced by the method of equal-channel elastic pressing as an example have shown that the effect of creep activation in SMC nickel related to the action of grain boundary diffusion flows of impurity atoms (copper) from the coating, which is estimated by the ratio $\dot{\varepsilon}_2/\dot{\varepsilon}_1$ ($\dot{\varepsilon}_1$ and $\dot{\varepsilon}_2$ are the velocities during the steady-state stage of creep of the SMC material in vacuum and under the conditions of diffusion of impurity atoms from the surface, respectively), takes place in the range of lower temperatures (398–473 K) compared to coarse-grained nickel (773–973 K) (Fig. 5).

Table 4 presents data on the effect of the temperature of preliminary annealing on the rate of creep of SMC nickel during the steady-state stage for creep in vacuum and under the conditions of diffusion of copper atoms from the surface. From Table 4 it can be seen that as the temperature of preliminary annealing is increased, and, hence, the energy of GB's is decreased, the steady-state creep rate in vacuum for SMC nickel increases and the effect of creep activation due to the action of diffusion flows of impurity atoms from the surface decreases to zero. As this takes place, the apparent creep activation energy increases to the values characteristic of coarse-grained nickel.

Thus, the data cited testify that in SMC metals produced by methods of intense plastic deformation, a low-temperature anomaly is observed in grain boundary heterodiffusion at temperatures below $0.4T_{melt}$ which consists in an increase in coefficients and a decrease in activation energy of grain boundary heterodiffusion compared to the

TABLE 4. Creep Parameters for SMC Nickel and for the Ni(Cu) System at 423 K after Preliminary Annealings in the Temperature Range 398–673 K [32]

T_{anneal}, K	σ, MPa	Creep of Ni in vacuum			Creep of Ni(Cu) under diffusion of copper from the coating		
		$\dot{\varepsilon}$, s^{-1}	δ, %	$Q_c \pm 15$, kJ/mol	$\dot{\varepsilon}$, s^{-1}	$\delta \pm 0.5$ %	$Q_c \pm 15$, kJ/mol
398	630	$1.2 \cdot 10^{-6}$	5.4	115	$3.3 \cdot 10^{-6}$	6.3	70
423	630	$1.5 \cdot 10^{-6}$	6	112	$3.6 \cdot 10^{-6}$	7.2	84
473	630	$2.6 \cdot 10^{-6}$	8.4	117	$3.9 \cdot 10^{-6}$	9.2	121
573	515	$3.3 \cdot 10^{-6}$	14.4	171	$3.7 \cdot 10^{-6}$	15.2	190
673	385	$2.7 \cdot 10^{-6}$	22	268	$2.6 \cdot 10^{-6}$	20	274

corresponding values for coarse-grained polycrystals and which is due to the nonequilibrium state of grain boundaries formed during intense plastic deformation.

Anomalous high values of grain boundary diffusion coefficients compared to those typical of ordinary polycrystals were also detected in a number of experimental studies of NC materials with a mean grain size of about 10 nm [35–38] which were produced by condensation from a gas medium and by powder compaction. These anomalies are discussed elsewhere [39, 40].

By now, alongside with speculations as to a possible effect of the residual pores and vacancy clusters formed during the preparation of NC specimens, some physical models of the detected "anomalous" diffusion penetrability of grain boundaries in rather perfect SMC materials with a density close to that of bulk materials have been proposed. In the pioneering study of the self-diffusion in NC materials performed with copper as an example [35] it has been shown that the NC condition is characterized both by a higher diffusion mobility of atoms along GB's and by a lower activation energy compared to those typical of an ordinary polycrystal. Based on this observation, the conclusion has been made [35] that in the NC condition, the diffusion mechanism of mass transfer is dominant, and it is the same as the mechanism of surface diffusion. However, these investigations did not consider a possible effect of the diffusion over triple junctions of grains. At the same time, triple junctions make a considerable portion of the intergrain region in polycrystals with grain sizes ranging to several tens of nanometers [41], and the mobility of atoms in them is much greater than in grain boundaries owing to the excess volume at grain junctions [42].

Recently a model of diffusion for polycrystals has been proposed [43] in which the diffusion paths over the intergrain region include both grain boundaries and triple junctions. The use of this model for the calculation of the coefficient of triple junction diffusion by the data on self-diffusion in NC Cu, Ni, and α-Fe available in the literature has led to the conclusion that the triple junction diffusion rate is 3–5 orders of magnitude greater than the grain boundary diffusion rate in the temperature range $(0.17–0.29)T_{melt}$, and the corresponding activation energy of triple junction diffusion is comparable to that characteristic of liquid metals [40].

Comparison of the coefficients D_b for NC copper in the temperature range 300–400 K [39] and the coefficients D_b for macrocrystalline copper obtained by interpolation of new data on D_b for high-purity copper from temperatures of 700–1000 K [44] has been performed [39]. This comparison has shown that the rate of diffusion of copper atoms along the boundaries of nanocrystals produced by condensation from a gas medium and by powder compaction [35] is practically the same as that in the boundaries of well-annealed coarse-grained copper. The authors of Ref. 39 did not consider the effect of triple junctions on the diffusion rate. Estimation of the contribution of triple junction diffusion of copper in the supposition that the effective coefficient of intergrain diffusion coincides with that of grain boundary diffusion has led to the conclusion that the triple junction diffusion coefficient cannot be greater more than 10 times than the grain boundary diffusion coefficient [39].

To discuss this pronounced difference between the conclusions of the authors of Refs. 39 and 40, it is necessary to note that an analysis of diffusion experimental data should include model notions about the polycrystal structure and boundary conditions for the diffusion process. Results of diffusion experiments were processed till now based on a simple model of grain boundary diffusion [26] though this model does not describe the actual structure of grain

boundaries. This model is actively developed to take into account the complicated diffusion paths in an NC material [39, 40]; however, the approximations involved in the model should inevitably influence the interpretation of experimental data. Therefore, in analyzing the reasons for significant discrepancies, such as those above, independent data about the parameters of diffusion in NC materials obtained without considerations of model notions about the structure of the NC state should be of great importance. This possibility is provided by the computer simulation of NC copper on an atomic level owing to the small grain sizes (8 nm) in specimens for which actual diffusion experiments have been performed for this material [35] and to the existence of well approved potentials of interatomic interactions in copper [45] constructed in the framework of the embedded atom method.

DIFFUSION CHARACTERISTICS OF GB'S AND TRIPLE JUNCTIONS

To analyze experimental data on the diffusion in NC materials, the grain boundary diffusion coefficient D_{GB} and the triple junction (TJ) diffusion coefficient D_{TJ} [40] are usually introduced. In this case, D_{GB} and D_{TJ} are the parameters of the GB and TJ diffusion model. They are determined by the squared diffusion displacements of atoms, $\Delta \boldsymbol{r}_i$, using the Einstein expression for the coefficient of diffusion in a three-dimensional medium:

$$D = \frac{\sum_{i=1}^{N} (\Delta \boldsymbol{r}_i)^2}{6Nt}. \tag{7}$$

Here N is the number of atoms in the corresponding phase and t is the time for which the displacement of atoms took place. In the limit of long times, the slope of the function that describes the time dependence of the mean square of displacements of atoms is assumed to be a constant for the range under consideration. However, D_{GB} and D_{TJ} have no physical meaning outside the framework of the chosen model of GB and TJ diffusion. Therefore, to describe the diffusion in NC materials, some other characteristics are required, irrespective of the model notions about the GZ and TJ structure.

We shall restrict our consideration to self-diffusion, noting that the sum of the squared diffusion displacements of atoms in a material seams to be an additive quantity which increases proportionally to the number of atoms. Following the concept of excess additive quantities for characterization of defects, developed in thermodynamics, we can describe the self-diffusion in an NC material by the excess sum of squared diffusion displacements of atoms resulting from the formation of GB's and TJ's, in relation to the crystalline state. Then the rate of rise of the ΔZ excess of the sum of squared diffusion displacements of atoms in an NC specimen accumulated in a time t is represented as the sum of the GB and TJ contributions:

$$(\Delta Z / t) = \zeta_{GB} A_{GB} + \zeta_{TJ} l_{TJ}. \tag{8}$$

Here ζ_{GB} is the average excess sum of squared displacements of atoms per unit time that is related to the formation of a grain of the a grain boundary and referred to a unit area of the grain boundary and referred to a unit area of the grain boundary; ζ_{TJ} is the average excess sum of squared displacements of atoms per unit time that is related to the formation of a triple junction and referred to a unit length of the triple junction; A_{GB} and l_{TJ} are the summarized area of grain boundaries and the summarized length of triple junctions in the NC material, respectively. Note that in expression (8) by the quantity $(\Delta Z/t)$ is implied the slope of the function that describes the dependence of ΔZ on t which can be determined by analyzing diffusion experiments or computer simulation data.

From the definition of the diffusion coefficient (7) it follows that the introduced characteristics of GB's and TJ's can be related to the corresponding diffusion coefficients D_{GB} and D_{TJ} by the expressions

$$(D_{GB} - D_V)\delta = \frac{\Omega}{6}\zeta_{GB} \text{ and } (D_{TJ} - D_V)R^2 = \frac{\Omega}{6}\pi\zeta_{TJ} \tag{9}$$

if we assume that the GB and TJ are continuous phases shaped as a plate of thickness δ and a cylinder of radius R, respectively. Here D_V is the grain bulk diffusion coefficient and Ω is the mean volume per atom. We shall consider only the cases where the grain bulk diffusion is much less intense than the diffusion in the intergrain region, and therefore we shall assume that $D_V = 0$. This consideration is valid, for instance, for the diffusion in an NC material at low homologous temperatures [35, 37] and for a computer simulation of the diffusion process in NC metals for times within which the vacancy concentration in the grain bulk remains negligible and the diffusion by the vacancy mechanism has no time to develop. In this case, expressions (9) allow us to compare the diffusion characteristics obtained with a model approach (D_{GB} and D_{TJ}) and without resort to such an approach (ζ_{GB} and ζ_{TJ}). From relations (9) it can also be seen that the products $D_{GB}\delta$ and $D_{TJ}R^2$ are physically meaningful irrespective of the model notions about the structure of GB's and TJ's, and represent, within some factors, the rates of increase of the excess sum of squared diffusion displacements of atoms in relation to the crystalline state in GB's and in TJ's, respectively.

According to expression (8), to obtain ζ_{GB} and ζ_{TJ} with known $(\Delta Z / t)$ for nanocrystalline specimens, it is necessary to know the area of the GB's and the length of the TJ's and to find the relations between these quantities. To obtain the quantities A_{GB}, a procedure was proposed [48] which is based on the stereometric identity [46] $A / V = 2 / < L >$, where A is the summarized area of the GB's in the NC specimen not taking into account the region of triple junctions, V is the volume of the specimen, and $< L >$ is the mean grain size determined by the secant method (mean intercept length). The actual area of the GB's, A_{GB}, is less than A by the quantity δA, which is determined by the region of triple junctions and is calculated by considering the interaction of the triple junctions and the adjacent GB's. In the present work, this interaction is taken into account by the demand of local thermodynamic equilibrium in a neighbourhood of the triple junctions. The requirement of local equilibrium for a triple junction at constant pressure and temperature implies that the variations in Gibbs energy upon any infinitesimal rearrangements of the triple junction region to the GB region and upon reverse rearrangements are zero. From this follows a simple relation between the average energy of a triple junction and that of the n adjacent GB's:

$$nR\gamma_{GB} = 2\gamma_{TJ}, \tag{10}$$

if we assume that the triple junction region is a homogeneous phase shaped as a cylinder of radius R. In relation (10), γ_{GB} and γ_{TJ} are the specific energies of the GB and of the TJ, respectively. Assuming that the reduction in GB area δA is equal to nRl_{TJ} and using relations (8), (10) and the stereometric identity, we obtain a formula for the calculation of ζ_{TJ} and ζ_{GB}:

$$(\Delta Z / t)\frac{< L >^2}{V} = 2\zeta_{GB} < L > + \lambda\left(\zeta_{TJ} - \frac{2\gamma_{TJ}}{\gamma_{GB}}\zeta_{GB}\right). \tag{11}$$

Here λ is a dimensionless parameter which determines the dependence of the specific length of triple junctions on the mean grain size: $l_{TJ} / V = \lambda / < L >^2$. This parameter is equal to 3.03 for specimens with grains of the same size which fill a space with bcc packing and to 2.63 for specimens with grains of random size and shape [47, 48]. Expression (11) follows from the condition of local thermodynamic equilibrium of TJ's under any supposition about the shape of the TJ cross-section and does not depend on the number of GB's forming TJ's in different regions of the specimen, and the quantities γ_{GB} and γ_{TJ} are average specific energies of the GB's and TJ's in the specimen. According to formula (11), to calculate the intergrain diffusion parameters ζ_{GB} and ζ_{TJ}, it is necessary to know the values of $\Delta Z / t$ for a series of specimens with various mean grain sizes <L>. Then the GB diffusion parameter ζ_{GB} is determined from the slope of the linear function that describes the dependence of $((\Delta Z / t) / V) < L >^2$ on $< L >$, and the TJ diffusion parameter ζ_{TJ} is estimated from the intersection of this function with the axis of ordinates. Note that the estimation of the mean parameters of GB and TJ diffusion (ζ_{GB} and ζ_{TJ}) by this procedure does not require model notions about the geometric structure of GB's and TJ's.

Construction of model NC specimens. Now the most generally employed method of construction of model NC specimens [49] is that based on the procedure proposed by Voronoi. Following this method, a model specimen of NC metal is constructed by filling the volume of the computational cell with nanograins grown up of randomly localized and crystallographically oriented germs. Following the Voronoi procedure, the space is filled with atoms until the neighboring grains become overlapped. The resulting NC specimen is a collection of nanograins shaped as Voronoi's polyhedrons centered at the places of localization of grain germs. The specimen final state that is used in computations by the method of molecular statics at 0 K is attained by annealing at 300 K with the molecular dynamics method which is followed by cooling to 0 K. It is supposed that model NC specimens constructed in such a way represent the actual structure of NC metals produced by compaction. By now this method has been well approved by many authors in studying the properties of the NC state in metals ([50] and the cited publications).

In theoretical studies, the grain size in an NC specimen is generally characterized by the diameter D of a sphere whose volume is equal to the mean grain volume [49]. The quantity D is related to the mean grain size $< L >$ calculated by the secant method by the relation $D = 1.65 < L >$, which is exact in the case of grains of the same size whose centers form a bcc lattice. To calculate the GB and TJ diffusion characteristics, a series of 14 model NC specimens of copper with the mean size D ranging from 5.3 to 14.5 nm has been constructed. The specimens were constructed with the use of periodic boundary conditions; each specimen included 16 grains in a computational cell and the specimens with the largest grains consisted of 2 million atoms. To inhibit the grain growth at high temperatures during the simulation by the molecular dynamics method, the centers of Voronoi's polyhedrons were placed at the sites of the bcc lattice and an additional condition was imposed on the misorientations of neighboring grains whose angle was no less than 15°. Thus all grains in each model specimen had the same shape and volume and all GB's were large-angle. It has been shown [48] that the thermodynamic characteristics of GB's and TJ's in model specimens constructed by this method coincide with those in specimens with randomly chosen centers of Voronoi's polyhedrons; therefore, the chosen grain shape does not make the simulation results less general. On the other hand, in the case of random grain shapes, the grain structure is rearranged at high temperature during the simulation, and this does not allow one to determine the diffusion characteristics by the method described above.

Simulation results. The computer experiment on the determination of the sum of squared diffusion displacements of atoms in the 14 NC specimens of copper described above was performed by the method of molecular dynamics (MD). The simulation was carried out at high homologous temperatures varied from 950 to 1200 K within $\sim 10^2$ ps because of the limitedness of the accessible time of the MD experiment. This time was long enough for the development of diffusion processes in the high-temperature mode. The MD step was 3 fs. Before the conduction of the model experiment, each specimen was kept at a given temperature and zero pressure for 24 ps by the MD method with the use of algorithms described elsewhere [51, 52]. Then the external actions were switched off and the simulation was carried out by the NVE (constant number of particles, volume, and total energy) MD scheme. The squared displacements of atoms (SDA's) were computed 9 ps later, and their values were stored in every 0.3 ps. The sum of squared diffusion displacements of atoms ΔZ (displacements for distances more than $0.35a_0$, where a_0 is the lattice constant for copper) accumulated in a time t was averaged over 20 initial points in time. The function that describes the dependence of ΔZ on t was constructed within 120 ps; it is shown in Fig. 1 for a model specimen of copper with the mean grain size D = 9.7 nm and the computational cell including 603894 atoms. As can be seen from Fig. 1, the chosen parameters of the model experiment provide a clear linear dependence of ΔZ on t at all temperatures considered. The error of the computation of $(\Delta Z/t)$ was no more than 0.2% for all model experiments performed. During the simulation, vacancies were formed near the GB and migrated in the grain bulk. For instance, after the simulation, in the specimen with the least mean grain size of 5.3 nm, 8 vacancies were revealed at a temperature of 1200 K, 4 vacancies at 1000 K, and 1 vacancy at 950 K. In this case, the contribution of tre bulk diffusion to $(\Delta Z/t)$ at 950 K was 2 orders of magnitude lower than the error of determination of $\Delta Z/t$, and at 1200 K it was half that, provided that the number of vacancies detected in the specimens persisted throughout the computer experiment. This makes it possible to neglect the contribution of the bulk diffusion and to use the method developed for a quantitative description of GB and TJ diffusion.

TABLE 5. Predicted and Experimental Values of the Parameters of the Arrhenius Relation Between $D_{GB}\delta$ and Temperature for High-Purity Copper

	ΔE_{GB}, eV/at.	P_0
Experiment [44] 784–973 K	99.999%	
	0.87	$1.16 \cdot 10^{-15}$
Experiment [44] 720–1066 K	99.9998%	
	0.75	$3.89 \cdot 10^{-16}$
Simulation 950–1200 K	100%	
	0.70 ± 0.03	$(2.4 \pm 0.9) \cdot 10^{-16}$

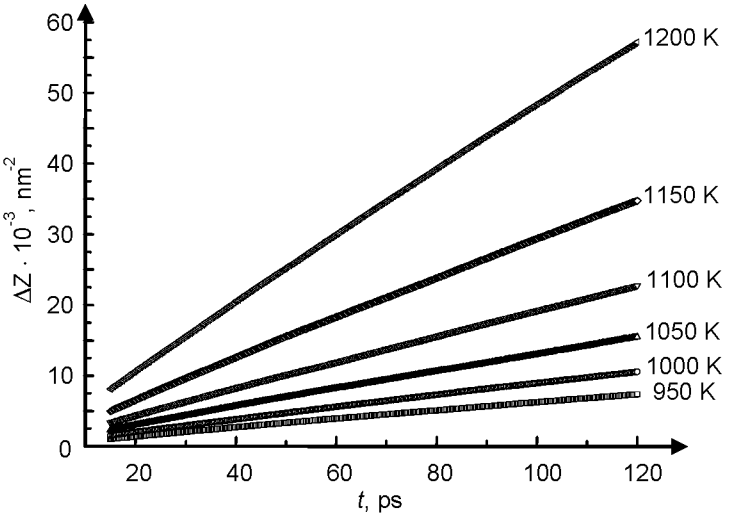

Fig. 6. Average sum of squared diffusion displacements of atoms, ΔZ, versus the time of the computer experiment for an NC specimen of copper with the mean grain size D = 9.7 nm at temperatures varied from 950 to 1200 K.

Analysis of the computer experiment performed by the method proposed is presented by the data in Table 5 and in Fig. 6. In Table 5, the parameters ΔE_{GB} and P_0 of the Arrhenius relation $D_{GB}\delta = P_0 \exp(-\Delta E_{GB} / k_B T)$ calculated from the values of ζ_{GB} and the same parameters obtained by analyzing the data of diffusion experiments for high-purity macrocrystalline copper [44] are compared. Comparison show very good agreement both for the self-diffusion activation energy ΔE_{GB} and for the preexponential factor P_0. This testifies, first, that the GB diffusion characteristics are identical for NC and for macrocrystalline copper at high temperatures and, second, that both the computer simulation predictions and the data of diffusion experiments presented in Table 5 are reliable.

Figure 7 presents the calculated contributions of TJ's to the excess sum of squared diffusion displacements of atoms for NC copper in relation to the crystalline state. Here, the relation between the mean grain size and the fraction f of the intergrain region occupied by triple junctions, according to a composite model of an NC material [53], is given from which follows $f = \delta / D$. We estimated the GB thickness δ as the diameter of the triple junction, whose value, 0.6 nm, follows from the above condition for a triple junction to be in equilibrium. Note that this value is close to 0.5 nm, the value that is often taken for the GB thickness in model considerations of GB diffusion [40]. As can be seen from Fig. 7, the contribution of TJ's to intergrain diffusion is substantially greater than the simple estimates based on the geometrical notions about the region of triple junctions as being mere intersections of grain-boundary homogeneous phases. For grains 10 nm in size and for temperatures of about 900 K, this contribution is about four times greater than

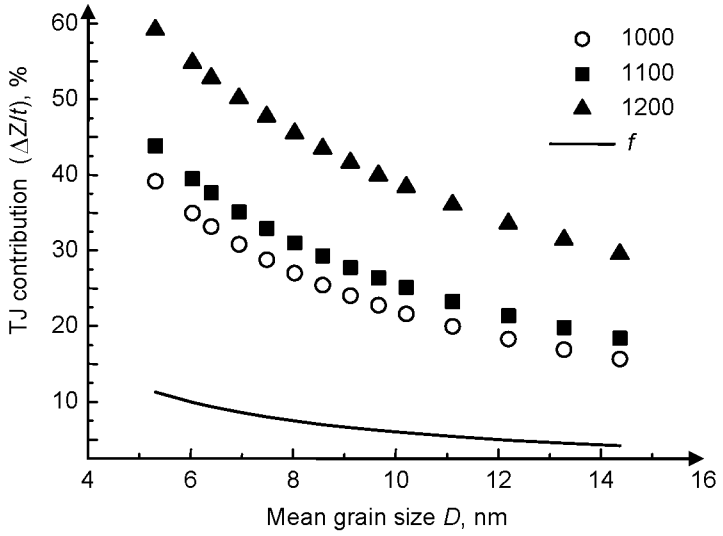

Fig. 7. Predicted contribution of triple junctions to the excess sum of squared diffusion displacements of atoms in NC copper versus mean grain size.

the respective estimates. The increase of this contribution with temperature can be accounted for by the much stronger effect of high temperatures on the thermal disorder of TJ's compared to GB's. This suggests that the diffusion paths over triple junctions should be considered in developing a model of diffusion in NC materials, such as the model described elsewhere [40]. However, as can be seen from Fig. 7, the contribution of TJ's, at least for high-temperature self-diffusion in NC copper, is not dominant compared to grain boundary diffusion. Therefore, it cannot result in "anomalous" intense diffusion in NC copper, as supposed by the authors of Ref. 40, at least in the range of high homologous temperatures. The TJ-to-GB diffusion coefficient ratios D_{TJ} / D_{GB} calculated by expressions (9) vary from 4.7 at a temperature of 950 K to 10.7 at 1200 K. This confirms the supposition of the authors of Ref. 39 that for copper this ratio is less than 10. However, the problem of the part played by triple junctions in the self-diffusion in NC copper at temperatures ranging between 300 and 400 K remains open. The solution of this problem, which is of principle as to diffusion processes in NC metals, can be obtained by performing diffusion experiments with a series of NC copper specimens with different mean grain sizes and then analyzing the results by the method proposed above which does not use model notions about the structure of GB's and TJ's. The above procedure of processing of diffusion experiments cannot substitute model approaches, especially in studying heterodiffusion. This procedure can be used in performing critical experiments aimed at solving some special problems, such as the problem of the part played by triple junctions in the diffusion in the intergrain region.

Direct atomic-level simulation of diffusion processes in SMC materials produced by IPD is impossible for reasons of the complexity of their atomic structure and of the relatively large grain sizes. However, methods of computer simulation on the atomic level allow one to reveal general features in the variations of GB characteristics with an increase in GB-related excess volume δV from the data of investigations of model bicrystals. As the relevant relations are found, it becomes possible to interpolate the simulation predictions for SMC materials with the use of experimental values of the excess volumes δV for these materials. This approach was realized [54] to estimate the proportion between the grain boundary diffusion coefficients for SMC materials produced by IPD and for those not subjected to this treatment.

Estimates obtained from indirect measurements of diffusion coefficients and from predictions of computer simulations performed on the atomic level [54] confirm the data of direct measurements that show that the effective diffusion coefficients for the SMC state are several orders of magnitude greater than those for the coarse-grained state. Here it should be noted that the increased diffusion mobility of atoms in GB's of SMC materials is directly related to the increased GB energy in these materials, whereas the GB energies in NC materials produced by compaction coincide

with those in the macrocrystalline state [47, 48]. This is in compliance with the fact that the GB diffusion characteristics are the same for the NC and for the macrocrystalline state. Therefore, the increased effective diffusion coefficients for NC materials produced by compaction seam to be related only to the effect of triple junctions which occupy a comparatively larger space in a material with a smaller mean grain size.

CONCLUSION

The effective coefficients of grain boundary self-diffusion and heterodiffusion in submicrocrystalline and nanocrystalline metals at temperatures below $0.4T_{melt}$ are several orders of magnitude greater and the activation energy of grain boundary heterodiffusion is 1.5–2 times lower compared to the corresponding values for coarse-grained polycrystals.

Analysis of computer simulation predictions and experimental data on the self-diffusion along grain boundaries in copper has shown unambiguously that the parameters of grain boundary self-diffusion are the same for nanocrystalline and for macrocrystalline copper. Therefore, the anomalous increase in effective coefficients of self-diffusion in nanocrystalline materials produced by compaction seams to be related to the effect of triple junctions whose contribution to the diffusion process is more pronounced for smaller mean grain sizes.

The diffusion in submicrocrystalline materials produced by methods of intense plastic deformation features, compared to nanocrystalline materials produced by compaction, first of all, an increased diffusion penetrability of grain boundaries which is due to their nonequilibrium state resulting from intense plastic deformation.

The work has been supported in part by the Russian Foundation for Basic Research (Grant No. 06-02-17336) and by Presidium of the Russian Academy of Sciences (Project No. 2.7).

REFERENCES

1. Yu. R. Kolobov, R. Z. Valiev, G. P. Grabovetskaya, *et al.*, Grain Boundary Diffusion and Properties of Nanostructured Materials, Cambridge International Science Publishing, Cambridge (2007).
2. R. Z. Valiev and I. V. Aleksandrov, Nanostructured Materials Produced by Intense Plastic Deformation [in Russian], Logos, Moscow (2000).
3. Yu. R. Kolobov, Diffusion-Controlled Processes at Grain Boundaries and Plasticity of Metallic Polycrystals [in Russian], Nauka, Novosibirsk (1998).
4. H. Gleiter, Phys. Status Solidi, **172**, 41–52 (1992).
5. B. S. Bokstein, H. D. Brose, L. I. Trusov, and T. P. Khvostantseva, Nanostructured Materials, in: Proc. the 2nd Intern. Conf. on Nanostructured Materials, Stuttgard, 1995, pp. 873–876.
6. L. N. Larikov, Metallofizika i Noveishie Tekhnologii, **17**, 3–29 (1995).
7. P. Keblinski, D. Wolf, S. R. Phillpot, and H. Gleiter, Scripta Mater., **41**, 631–636 (1999).
8. B. Bokstein, M. Ivanov, Yu. Kolobov, and A. Ostovsky, J. Met. Nanocryst. Mater., **19**, 69–107 (2004).
9. R. Wurschum, A. Kubler, S. Gruss, *et al.*, Ann. Chim. Phys., **21**, No. 6/7, 471–482 (1996).
10. G. P. Grabovetskaya, I. V. Ratochka, Yu. R. Kolobov, and L. N. Puchkareva, Fiz. Met. Metalloved., **83**, No. 3, 112–116 (1997).
11. H. Tanimoto, P. Farber, R. Wurschum, *et al.*, Nanostructured Materials, **12**, 681–684 (1999).
12. H. Tanimoto, L. Pasquini, R. Prummer, *et al.*, Scripta Mater., **42**, 961–966 (2000).
13. K. P. Gurov, A. M. Gusak, V. V. Kondrat'ev, and F. A. Kotenev, Fiz. Met. Materialoved., **62**, 35–42 (1986).
14. I. Kaur, Yu. Mishin, and W. Gust, Fundamentals of Grain and Interphase Boundary Diffusion, Wiley, Chichester, New York, Toronto (1995).
15. L. Klinger and E. Rabkin, Acta Mater., **47**, 725–734 (1999).
16. B. S. Bokshtein and A. B. Yaroslavtsev, Diffusion of Atoms and Ions in Solids [in Russian], MISIS, Moscow (2005).
17. Yu. R. Kolobov, G. P. Grabovetskaya, M. B. Ivanov, *et al.*, Scripta Mater., **44**, 873–878 (2001).

18. Y. R. Kolobov, G. P. Grabovetskaya, K. V. Ivanov, *et al.*, in: Proc. Symp. on Ultrafine Grained Materials III, Charlotte, North Carolina, USA, March 14–18, 2004, pp. 621–628.
19. G. P. Grabovetskaya, I. P. Mishin, I. V. Ratochka, *et al.*, Pis'ma Zh. Tekh. Fiz., **33**, No. 4, 36–38 (2008).
20. Yu. R. Kolobov, G. P. Grabovetskaya, K. V. Ivanov, *et al.*, Solid State Phenom., **94**, 35–40 (2003).
21. O. A. Kaibyshev and R. Z. Valiev, Grain Boundaries and Properties of Metals [in Russian], Metallurgia, Moscow (1987).
22. G. P. Grabovetskaya, I. P. Mishin, Yu. R. Kolobov, *et al.*, Izv. Vyssh. Uchebn. Zaved., Fiz., No. 5, 37–42 (2007).
23. S. Friedman and J. Brett, TraCMK. Met. Soc. AIME, **242**, 2121–2125 (1968).
24. V. B. Marvin and Yu. R. Kolobov, Poverkhnost. Fiz., Khim., Mekh., No. 7, 131–139 (1991).
25. Yu. M. Mishin and I. M. Razumovskii, Structure and Properties of Internal Interfaces in Metals [in Russian], Nauka, Moscow (1988).
26. J. C. Fischer, J. Appl. Phys., **22**, 74–77 (1951).
27. Yu. I. Pochivalov, Yu. R. Kolobov, and A. D. Korotaev, Fiz. Met. Metalloved., **82**, 296–301 (1982).
28. Ya. E. Geguzin, Yu. S. Kaganovskii, and E. G. Mikhailov, Metallofizika, **9**, No. 5, 118–120 (1987).
29. D. Liu, W. A. Miller, and K. T. Aust, Acta Met., **37**, 3367–3378 (1989).
30. N. I. Noskova and R. R. Mulyukov, Submicrocrystalline and Nanocrystalline Metals and Alloys [in Russian], RAS UD Publishers, Ekaterinburg (2003).
31. Yu. R. Kolobov, G. P. Grabovetskaya, I. V. Ratochka, *et al.*, Ann. Chim. Sci. Mat., **21**, No. 3/4, 483–491 (1996).
32. G. P. Grabovetskaya, Fiz. Mezomekh., **8**, No. 2, 49–60 (2005).
33. A. H. King, Intern. Materials Rev., **32**, No. 4, 173–189 (1987).
34. Yu. R. Kolobov, V. B. Marvin, I. V. Ratochka, and A. D. Korotaev, Dokl. AN SSSR, **283**, 605–608 (1985).
35. J. Horvath, R. Birringer, and H. Gleiter, Solid State Commun., **62**, 319–322 (1987).
36. Z .B. Wang, N. R. Tao, W. P. Tong, *et al.*, Acta Mater., **51**, 4319–4329 (2003).
37. S. Schumacher, R. Birringer, R. Strauss, and H. Gleiter, Acta Metallurg., **37**, 2485–2488 (1989).
38. H. J. Hofler, R. S. Averback, H. Hahn, and H. Gleiter, J. Appl. Phys., **74**, 3832–3839 (1993).
39. S. V. Divinskii, S. M. Zakharov, and O. A. Shmatko, Usp. Fiz. Nauk, **7**, 1–39 (2006).
40. Y. Chen and Chr. A. Schuh, Scripta Mater., **57**, 253–256 (2007).
41. G. Palumbo, S. J. Thorpe, and K. T. Aust, Scripta. Metallurg. Mater., **24**, 1347–1350 (1990).
42. B. Bokstein, V. Ivanov, O. Oreshina, *et al.*, Mater. Sci. Eng. A., **302**, No. 1, 151–153 (2001).
43. Y. Chen and Chr. A. Schuh, J. Appl. Phys., **101**, 063524 (2007).
44. T. Surholt and Chr. Herzig, Acta Mater., **45**, 3817–3823 (1997).
45. Yu. M. Mishin, M. J. Mehl, D. A. Papaconstantopoulos, *et al.*, Phys. Rev., **B63**, 224106–224121 (2001).
46. S. A. Saltykov, Stereometric Metallography [in Russian], Metallurgia, Moscow (1970).
47. A. G. Lipnitskii, A. V. Ivanov, and Yu. R. Kolobov, in: Proc. 2nd Intern. Symp. on Physics and Mechanics of Large Plastic Strains, June 4–9, 2007, St. Petersburg, 2007, p. 37.
48. A. G. Lipnitskii, A. V. Ivanov, and Yu. R. Kolobov, in Proc. XVI Intern. Conf. on Physics of Strength and Plasticity of Materials, Samara, June 26–29, 2006, V. 1, pp. 190–196.
49. H. van Swygenhoven, D. Farkas, and A. Caro, Phys. Rev., **B62**, 831–838 (2000).
50. D. Farkas, E. Bringa, and A. Caro, *Ibid.*, **B75**, 184111 (2007).
51. W. G. Hoover, Phys. Rev. A., **31**, 1695–1697 (1985).
52. H. J. Berendsen, J. P. M. Postma, W. F. V. Gunsteren, *et al.*, J. Chem. Phys., **81**, 3684–3690 (1984).
53. H. S. Kim, Y. Estrin, and M. B. Bush, Acta Mater., **48**, 493–504 (2000).
54. Yu. R. Kolobov, I. V. Ratochka, K. V. Ivanov, and A. G. Lipnitskii, Izv. Vyssh. Uchebn. Zaved., Fiz., No. 8, 49–64 (2004).